Urea Metal-organic Frameworks for Nitro-substituted Compounds Sensing

*Alireza Azhdari Tehrani,[a] Leili Esrafili,[a] Sedigheh Abedi,[a] Ali Morsali,[*a] Lucia Carlucci[b] Davide M. Proserpio,[b,c] Jun Wang,[d] Peter C. Junk,[d] and Tianfu Liu,[e]*

[a]*Department of Chemistry, Faculty of Sciences, Tarbiat Modares University, P.O. Box 14115-175, Tehran, Iran. E-mail: Morsali_a@modares.ac.ir;*

[b]*Dipartimento di Chimica, Università degli Studi di Milano, Milano 20133, Italy*

[c] *Samara Center for Theoretical Materials Science (SCTMS), Samara University, Samara 443086, Russia*

[d] *College of Science & Engineering, James Cook University, Townsville Qld, 4811, Australia*

[e] *Department of Chemistry, Northwestern University, 2145 Sheridan Road, Evanston, Illinois 60208-3113, USA*

Abstract

Urea groups are known to form strong hydrogen bonds with molecules containing atom(s) that can act as hydrogen bond acceptor(s). Thus, urea is a particularly interesting building block for designing receptors for neutral or charged guests. In the quest for new sensors with enhanced performance for the detection of nitro-substituted compounds, two pillared metal-organic frameworks containing urea functional groups were synthesized and structurally characterized. The sensing properties of these frameworks toward nitro-analytes was investigated and compared to each other. The study clearly reveals the importance of urea groups orientation inside the pore cavity of MOFs, as well as the supramolecular interactions between the interpenetrated networks. This work is interesting as it represents the first example of urea-functionalized MOFs for nitro-analytes recognition.

Introduction

Metal-organic frameworks (MOFs) are a class of porous materials with great potentials in catalysis,[1] gas storage[2] and sensing.[3] An important feature of MOFs over other porous materials is the ability to tune their pore size, topology and functionality by the deliberate design and selection of organic and inorganic molecular building blocks from which the network is constructed.[4] Taking advantage of this feature, chemists have tried to design and synthesize novel MOFs having particularly desired and predetermined functions and properties. In this regard, recently, many efforts were focused on the selective molecular recognition and detection of small molecules,[5] cations[6] and anions[7] by MOFs. Much attention has been given in recent years to the selective sensing and removal of nitroaromatic compounds (NACs) owing to security, environmental and humanitarian issues.[8-11] Thus, exploring novel sensors for the detection of NACs, such as nitrobenzene, 2,4-dinitrotoluene (2,4-DNT) and 2,4,6,-trinitrotoluene (TNT) has become an urgent issue and is the subject of intensive research.[12-13] More interestingly, it has been shown that incorporating supramolecular recognition units into the MOF backbone has enabled the docking of specific guests and is advantageous to create specific responses.[14-15]Among the MOFs reported to date, MOFs containing urea, thiourea and squaramide groups are currently in the spotlight due to their potential use as a promising biomimetic alternative to Lewis acid catalysis.[16-21] The appealing idea of incorporating a double hydrogen-bond donating (HBD) site that is prone to self-quenching into MOFs was proposed by Farha, Hupp, Scheidt and co-workers.[22-23] They have investigated the catalytic activity of the urea-based MOF for the Friedel–Crafts reaction between pyrroles and nitroalkenes. Soon after this report, supramolecular chemists became more interested in hydrogen-bonding organocatalysts immobilized on MOFs aiming to the development of hydrogen-bonding organocatalysts for complicated chemical transformations. [16-20, 24-25] Urea groups are known to form strong hydrogen bonds with the molecules containing atom(s) that can act as hydrogen bond acceptor(s).[26-27] Thus, urea is a particularly interesting building block for designing receptors for neutral or charged guests.[28-30] In the quest for new sensors with enhanced performance for the detection of NACs, we are currently interested in evaluating the potential of urea-MOFs as hydrogen bond donating receptors. Herein, we introduce two urea-containing MOFs, TMU-31 and TMU-32, which are formed by using the 4,4'-(carbonylbis(azanediyl))dibenzoic acid (L1), 1,3-di(pyridin-4-yl)urea (L2) ligands and 4,4′-oxybis(benzoic) acid (H_2oba), 1,3-di(pyridin-4-yl)urea (L2) ligands, respectively, and $Zn(NO_3)_2 \cdot 6H_2O$ under solvothermal conditions. The sensing properties of these two frameworks toward nitro-analytes were investigated and compared to each other. The study

reveals the importance of urea groups orientation inside the pore cavity of MOFs, as well as the supramolecular interactions between the interpenetrated networks.

Experimental Section

Synthesis

L1 and L2 were synthesized according to the procedures described in the supporting information, Figures S1 and S2.

Synthesis of TMU-31

0.298 g of $Zn(NO_3)_2.6H_2O$ (1 mmol), of 0.3 g L1 (1 mmol) and 0.214 g of synthesized L2 (1 mmol) were dissolved in 15 ml of *N*,*N′*-Dimethylformamide (DMF). The mixture was then placed in Teflon-lined stainless steel autoclaves and heated to 100 °C for 3 days. The mixture was then gradually cooled to room temperature over 48 hours. Colorless crystals were formed on the walls of the container with a 45% synthesis yield. FT-IR data (KBr pellet, cm^{-1}): selected bands: 3359 (w), 2929 (w), 1665 (vs), 1599 (s), 1518 (s), 1382 (m), 1303 (w), 1182 (m), 1022 (w), 841 (w), 783 (w), 535 (w). Anal. calcd for $C_{29}H_{27}N_7O_7Zn$: C, 53.51; H, 4.18; N: 15.06, found: C, 53.58; H, 4.32, N: 15.14.

The trapped guest molecules can be removed by exchanging TMU-31 with acetonitrile followed by heating to get the guest-free form. The activation is confirmed by FT-IR spectroscopy, elemental analysis and powder X-ray diffraction. The absence of the peak at 1665 cm^{-1} in the FT-IR spectrum of activated sample confirms the removal of DMF molecules after activation.

FT-IR data (KBr pellet, cm^{-1}): selected bands: 3359 (w), 2929 (w), 1599 (s), 1518 (s), 1382 (m), 1303 (w), 1182 (m), 1022 (w), 841 (w), 783 (w), 535 (w). Anal. calcd for $C_{26}H_{20}N_6O_6Zn$: C, 54.04; H, 3.49; N: 14.54, found: C, 53.92; H, 3.54, N: 14.48.

Synthesis of TMU-32

0.298 g of $Zn(NO_3)_2.6H_2O$ (1 mmol), 0.258 g of H_2oba (1 mmol) and 0.214 g of L2 (1 mmol) were dissolved in 15 ml of *N*,*N′*-Dimethylformamide (DMF). The mixture was then placed in Teflon-lined stainless steel autoclaves and heated to 100 °C for 3 days. The mixture was then gradually cooled to room temperature over 48 hours. Colorless crystals were formed on the walls of the container with a 38% synthesis yield. FT-IR data (KBr pellet, cm^{-1}): 3287 (w), 2928 (w), 1738 (m), 1675 (s) 1597 (vs), 1513 (s), 1387 (m), 1292 (m), 1237 (w), 1181 (vs), 1020 (m), 833 (m), 657 (w), 532 (w).

Anal. calcd for $C_{31}H_{34}N_6O_9Zn$: C, 53.19; H, 4.90; N: 12.01, found: C, 53.14; H, 4.96, N: 11.95.

The trapped guest molecules can be removed by centrifuging several times with toluene followed by heating to get the guest-free form. The activation is confirmed by FT-IR spectroscopy, elemental analysis and powder X-ray diffraction. The absence of the peak at 1675 cm^{-1} in the FT-IR spectrum of activated sample confirms the removal of DMF molecules after activation.

FT-IR data (KBr pellet, cm^{-1}): 3290 (w), 2927 (w), 1740 (m), 1597 (s) 1516 (s), 1389 (m), 1293 (m), 1237 (w), 1181 (vs), 1021 (m), 833 (m), 658 (w), 530 (w).

Anal. calcd for $C_{25}H_{18}N_4O_6Zn$: C, 56.04; H, 3.39; N: 10.46, found: C, 56.12; H, 3.48, N: 10.42.

Results and Discussion

Crystal structure analysis of TMU-31 and TMU-32

TMU-31, [Zn(L1)(L2)]•DMF, was synthesized by combining $Zn(NO_3)_2 \cdot 6H_2O$, the L1 and L2 urea-based ligands using the solvothermal method at 100°C for 72 h to give X-ray quality crystals. X-ray crystallography reveals that TMU-31 crystallizes in the monoclinic $P2_1/c$ space group. In this compound, the coordination geometry around the Zn(II) can be described as distorted square pyramidal with the five coordination sites occupied by three oxygen atoms of carboxylate groups from two different L1 ligands with different coordination modes (κ^1*O* and κ^2 *O,O'*) and two pyridyl nitrogen atoms from two different L2 ligands. One of these pyridyl nitrogen atoms is located in the apical position, while the remaining pyridyl nitrogen atom and carboxylate oxygen atoms form the basal plane, Figure S1. An ORTEP view with labeling scheme showing the asymmetric unit and coordination environment about Zn1 is reported in Figure S3. Each Zn(II) center can be taken as a 4-connecting node being coordinated to four other Zn(II) atoms through two L1 and two L2 bridging ligands.

Structural analysis reveals that the urea N-H groups of L2 ligands form bifurcated hydrogen bonds with a carboxylic oxygen atom of each L1 ligand (N1···O7=2.870 Å; N2···O7=2.888 Å). In contrast, the urea N-H groups of L1 ligands are involved in N-H···O hydrogen bonds with the oxygen atom of the guest *N*,*N*-dimethylformamide (DMF) molecules (N4···O5=2.776 Å; N5···O5=2.872 Å).

TMU-32, [Zn(oba)(L2)]•2DMF•H_2O (H_2oba: 4,4'-oxydibenzoic acid; L2=1,3-di(pyridin-4-yl)urea), was synthesized by combining $Zn(NO_3)_2 \cdot 6H_2O$, the H_2oba ligand and L2 urea-based pillaring ligand

using the solvothermal method at 100°C for 72 h to give suitable X-ray quality crystals. TMU-32 crystallizes in the triclinic system, space group $P\bar{1}$. The asymmetric unit contains two oba ligands, two L2 ligands and two zinc atoms (Zn1 and Zn2). Zn1 has a distorted tetrahedral environment coordinating two different L2 ligands *via* the pyridyl groups, and two different oba ligands *via* the κ^1O carboxylate groups. Zn2 is pentacoordinate interacting with the second nitrogen atoms of the two L2 ligands and with the second carboxylate groups of the same two oba anions, one as unidentate (κ^1O) and the other as chelating (κ^2OO'). An ORTEP view with labeling scheme showing the asymmetric unit and coordination environment about Zn1 and Zn2 is reported in Figure S4.

Although the reactivity of H_2oba in combination with bridging pyridyl ligands has been largely explored no structures of mixed oba/L2 ligands are known. On the other hand mixed carboxylic/1,3-di-4pyridylurea ligands are very few and only two coordination networks have been found in the CSD containing L2 and dicarboxylate anions. These are [Zn{4-carboxylatobenzoyl)amino]benzoato}(1,3-dipyridin-4-ylurea)] (refcode: SOPLIU) and [Zn(biphenyl-4,4'-dicarboxylato)(1,3-dipyridin-4-ylurea)] (refcode: SOPLOA) showing 3D 4-fold interpenetrated **dia** networks.[31]

Topological Analysis of TMU-31 and TMU-32

Topological analysis of the resulting 3D framework of **TMU-31** reveals that it is an 8-fold interpenetrated diamondoid (**dia**) network. The distorted diamondoid cage of a single **dia** network, illustrated in Figure 1, shows elongation along the crystallographic *a* axis. The intracage Zn···Zn···Zn angles deviate from the ideal value of 109.5° and are spread in the range 90.7° - 125.3°, while distances between opposite Zn···Zn atoms are comprised in the range 23.5-46.4 Å. The huge void space comprised in a single diamondoid cage support the interpenetration of eight equal nets. The topology of interpenetration show class IIIa for TMU-31, that is four nets are related by translation along [1 0 0] while a center of inversion double the set resulting in 4+4 = 8-fold, Figure 2. Despite that **dia** underlying topology is the most commonly observed in coordination networks only 22 8-fold structures are known to ToposPro database,[32] moreover only two structures show interpenetration of class IIIa.[33-34]

The structure of **TMU-32** is a 2D layer that can be described as formed by the superposition of two hexagonal layers of composition $Zn1Zn2(oba)_3(L2)_2$ interconnected by coordination of one type of L2

ligand to the Zn1 and Zn2 atoms of the two hexagonal layers. From a topological point of view the 2D net is uninodal 4-connected with point symbol ($4^3.6^3$), topological type (6,3)Ia (see Figure 3).[35-36]

The thickness of a single layer, evaluated as the Zn1-N5···N8-Zn2 distance supported by the pillaring L2 ligand, is 14.3 Å. The irregular hexagonal windows show three different Zn1···Zn2 edges as a consequence of the different bridging ligands and their respective conformations. In particular, two edges are defined by the bridging L2 ligands (Zn1-N1···N4-Zn2) and are of 14.1 Å, a value similar to the thickness distance, showing similar conformations for the two different L2 ligands (the dihedral angles between the phenyl rings within each ligand are 15.2° and 2.4° for the edge and the pillaring L2 ligands, respectively). The other four Zn1···Zn2 edges are equal two by two and correspond to 13.9 Å and 14.8 Å being supported by bridging bis unidentate (μ- κ^1O, κ^1O') and unidentate-chelating (μ- κ^1O κ^2O',O'') oba ligands, respectively. The corresponding dihedral angles between the phenyl rings within each ligand are 83.9° and 86.9° (see Figure 3a). The layers are perpendicular to [1,-2,0] direction and, interestingly, are polycatenated in a parallel fashion to give an overall 3D array. Every thick layer result to be catenated with four other adjacent layers, two above and two below giving a Density of catenation (Doc) of 4 and an Index of separation (IS) of 2 (see Figure 4).[37]

Although this topological type has been found in many structures (163 coordination networks according to ToposPro database), entangled structures of (6,3)Ia layers are quite rare and to the best of our knowledge only two cases have been reported.[37] Among the 163 not entangled examples one of the first recognized (6,3)Ia coordination layers was found in $[RuCl_2(pyz)_4Ag](SO_3CF_3)$ (pyz = pyrazine; Refcode: XOHTOD), reported by some of us in 2002,[38] while one of the oldest examples recognized by TOPOS can be found in the crystal structure of cadmium maleate dihydrate published in 1974 (refcode: CDMALD).[39] The two known examples of entangled (6,3)Ia layers are $\{[Zn_2(TPOM)(1,4\text{-chdc})(NO_3)_2](H_2O)_2\}_n$ (TPOM =tetrakis(4-pyridyloxymethylene)methane, chdc=1,4-cyclohexanedicarboxylic acid, refcode: QOVDAI)[40] and $[Cd_2(hydeten)_2Ag_4(CN)_8].H_2O$ (hydeten: N-(2-hydroxyethyl)ethylenediamine, refcode: TOMBUU),[41] the first showing two fold interpenetration and the latter parallel polycatenation as the structure reported here but with a simpler entangled pattern with Doc=2 and IS=1. A comparison between the two parallel polycatenated structures (TOMBUU and the present structure) provides some differences mainly concerning the thickness, significantly shorter in TOMBUU being 10.8 Å, and the shape of the hexagonal windows that are rectangular with lateral size of 10.8×21.6 Å. These differences can account for the lower Doc and IS values found in TOMBUU. It should be noted that parallel polycatenation with Doc=4 and IS=2 is a quite rare

entanglement observed in only a handful of examples.[36] All the topological analysis has been done with ToposPro.[32] A deeper structural analysis for TMU-32 also shows bifurcated hydrogen bonds between the two N-H bonds of the urea fragment of L2 ligands and the carbonyl groups of μ-κ^1*O*κ^1*O'* oba ligands (N3···O7=2.858 Å; N2···O7=2.745 Å; N6···O10=2.818 Å; N7···O10=2.860 Å). These hydrogen bonds involve adjacent layers of the polycatenated array and if taken into account give a unique complex 3D supramolecular network.

Thermal analysis, activation and porosity of TMU-31 and TMU-32

TMU-31 shows limited porosity with the calculated void space per unit cell for guest-free framework of 25.1% (758.3 Å^3).[42] Also, the BET measurement showed that this compound is nonporous toward N_2. Thermogravimetric analysis (TGA) reveals that the hydrogen bonded DMF molecules are released from the network upon heating to about 230˚C, which causes ~11.5% weight loss of the material. The second weight loss observed starting at 250˚C corresponds to the decomposition of the framework, Figure S5. In order to activate the potential interacting sites of TMU-31, the DMF molecules within the porous structure could be exchanged with acetonitrile molecules, which are more easily removed. The activation process consists of immersing the as-synthesized crystals in acetonitrile for 3-days. After this, the sample was filtered and vacuum-dried at 60˚C for 4 h. The FT-IR spectroscopy, elemental analysis, and powder X-ray diffraction (PXRD) confirmed the removal of guest DMF molecules accommodated in the pores of the framework, Figures S6 and S8.

Thermogravimetric analysis (TGA) reveals that TMU-32 undergoes residual solvent loss between 100-120˚C (~2% weight loss) and 120-290˚C (~20% weight loss), followed with the decomposition starting at 320˚C, Figure S5. The trapped guest molecules can be removed by exchanging TMU-32 with toluene followed by heating to get the guest-free form. The activation is confirmed by FT-IR spectroscopy, elemental analysis and powder X-ray diffraction, Figures S7 and S9. The calculated void space per unit cell for guest-free TMU-32 framework is 33.9% (1081.6 Å^3).[42] The BET measurement showed that this compound is porous toward N_2 at 77 K; Brunauer−Emmett−Teller (BET) surface area of 432 m^2/g], Figure S10.

Nitro-substituted compounds sensing

Urea can donate two parallel hydrogen bonds to two oxygen atoms of oxoanions, such as NO_3^-,[43-47] or nitroaromatics, forming an eight membered ring.[48-52] TMU-31 and TMU-32 have been designed to study the host–guest interactions of the urea functionalized metal-organic frameworks with Y-shaped anions or nitro-substituted aromatics. Both TMU-31 and TMU-32 are based on zinc nodes. Similar to TMU-31, in TMU-32, the urea NH groups of pillaring linker (L2) are mainly involved in N-H···O hydrogen bonds with a carboxylic oxygen atom of the oxygen-donating ligand. In contrast, the urea group of L1 ligand in TMU-31 is H-bonded to the DMF guest molecules, Figure 5.

Nitroaromatics are oxidizers due to a low-lying unoccupied π* orbital, which can accept an electron from the excited state fluorophore, thus efficiently quenching the fluorescence emission of this compound.[53] Fluorescence quenching of nitroaromatics based on π-interactions, namely π···π stacking and C−H···π interactions, has been the subject of numerous investigations.[54-56] Accordingly, chemists have designed a variety of molecular receptors based on aromatic groups, which favor π-π stacking interactions between MOF and nitro-analytes. [5, 10, 57-60] In this regard, we have been interested in evaluating the potential of urea-functionalized MOFs as hydrogen bond donating receptors for nitroaromatics recognition. The fluorescence properties of both compounds were first investigated by immersing activated TMU-31 and TMU-32 in six different solvents, namely toluene, benzene, dimethylformamide, hexane, acetone and nitrobenzene, Figures S11-S14. As shown in Figures S13 and S14, benzene and toluene display a negligible effect on the emission of these compounds. Both frameworks show complete fluorescence quenching when they are immersed in nitrobenzene, with a quenching efficiency of >98% for both compounds. These MOFs exhibit fluorescence at 410 and 390 nm upon excitation both at 320 nm, for TMU-31 and TMU-32, respectively. Nitrobenzene (NB), 1,3-dinitrobenzene (1,3-DNB), 2,4-dinitrotoluene (2,4-DNT), 2,4,6-trinitrotoluene (TNT) and nitromethane (NM) were chosen to study the response of TMU-31 and TMU-32 towards nitroaromatics, Figures 6(a) and S15-S24. For both frameworks, the quenching efficiency is in the order of 1,3-DNB>2,4-DNT>NB>NM>TNT.

The Stern−Volmer (SV) quenching constants (K_{SV}) for both compounds were obtained by monitoring the fluorescence intensity response of the MOFs at different concentrations of the analytes. For TMU-31 and TMU-32, the Stern-Volmer plots predict linear dependence on quencher concentrations, with K_{SV} of 8.39×10^3 M^{-1}, 1.18×10^4 M^{-1}, 1.05×10^4 M^{-1}, 3.06×10^3 M^{-1} and 7.59×10^3 M^{-1} for NB, 1,3-DNB, 2,4-DNT, TNT and NM respectively, for TMU-32. For TMU-31, the K_{SV} values are as follows: NB=1.17×10^4 M^{-1}, 1,3-DNB=2.12×10^4 M^{-1}, 2,4-DNT=1.31×10^4 M^{-1}, TNT=5.58×10^3 M^{-1} and

NM=9.01×10^3 M^{-1}. The higher K_{SV} values in the TMU-31 compared to those in the TMU-32 indicate that the fluorescence quenching in the presence of TMU-31 is faster and more efficient than that of TMU-32, Figures S25 and S26. The K_{SV} values for nitroaromatics quenching by TMU-31 and TMU-32 are higher than some reported MOFs, which take advantage of π-interactions for nitro-analytes recognition.[5, 8, 11, 61-66] The photo-induced electron transfer (PET) mechanism may be involved in quenching the fluorescence since a linear fluorescence quenching response/concentration relation is obtained and the absorption band of the analyte has no effective overlap with the emission band of the fluorophore.[11, 67]

Since urea functional group can interact effectively with the hydrogen bond acceptors through chelate N-H···O hydrogen bonding, it is interesting to evaluate the nitroaromatics sensing ability of both frameworks in a solvent containing a hydrogen bond acceptor group (C=O). To get insight into this problem, we studied the fluorescence quenching properties of TMU-31 and TMU-32 toward NB and DNB in acetone as a solvent. The results showed a significant decrease of both frameworks responses to NB and DNB, Figures S27-S35. Interestingly, in the presence of acetone, TMU-32 responses faster and more efficient than TMU-31, with the K_{SV} values of NB= 460 M^{-1}, DNB=1109 M^{-1} and NB= 837 M^{-1}, DNB=1133 M^{-1} for TMU-31 and TMU-32, respectively. It can be concluded that the N-H···O hydrogen bonds may be the main host-guest interactions and in the presence of acetone there is a competition between solvent and nitroaromatic molecules for the receptor site. PXRD patterns and SEM images after nitroaromatics sensing are shown in Figures S8-S9 and S36-S37, indicating the retention of the framework of TMU-31 and TMU-32 after the nitroaromatics recognition. The inductively coupled plasma (ICP) analysis and Atomic Absorption Spectroscopy (AAS) were also used to investigate the framework stability. According to the ICP and AAS analyses, 0.48% of residual zinc was identified which significantly confirmed that more than 99% of the zinc metal center does not leach into the solution. Also, the fluorescence sensing ability of both frameworks was examined by the addition of different organics to the suspension of the complex. As shown in Figure 6b, the fluorescence of these compounds quenched effectively by nitroaromatic compounds, while with the addition of the same amount of organics (60 ppm in toluene), including benzene, chlorobenzene, phenol, anisole, ethanol, chloroform, tetrahydrofuran, acetonitrile and butylamine, the maximum change in the emission intensity was negligible, Figure S38. These frameworks was regenerated and reused for three cycles by centrifuging the dispersed solution after nitrobenzene sensing and washing the dispersed solution after use and washing several times with methanol, Figure 6c. In subsequent

studies, the applicability of TMU-31 and TMU-32 for the extraction and preconcentration of nitrobenzene and nitromethane, followed by their determination by gas chromatography–mass spectrometry (GC–MS) was investigated, Figure S39. The results revealed that TMU-31 has greater extraction efficiency (ER) (ER for NM=58.0% and ER for NB=42.6%) than TMU-32 (ER for NM=27.5% and ER for NB=26.6%), because of the more efficient interactions between TMU-31 and nitro-analytes, Table S1. It is to be noted that the MOF–analyte interaction may be a combination of partial entry of the analyte into the MOF pores and surface binding.

Moreover, to further understand the fluorescence quenching properties of both frameworks, the frontier molecular orbitals of nitro-analytes and MOFs were calculated using DFT at the generalized gradient approximation Perdew-Burke-Ernzerhof (GGA-PBE) level of theory, which has been shown to provide excellent descriptions of both molecular and solid state systems. [13, 68] DFT calculations confirmed that the conduction band minimums (CBM) of both TMU-31 and TMU-32 are higher in energy than the LUMO levels of nitroaromatics and the order of LUMO levels of nitroaromatics is TNT>1,3-DNB>2,4-DNT>NB>NM, thus predicting that the excited electron from the CBM of MOF is transferred to the LUMO of the nitro-analytes, Figure 7. It is to be noted that the relative quenching efficiencies are not fully in accordance with the calculated LUMO energies of nitro-analytes, as it cannot account for the effect of interactions between the frameworks and molecules. The interaction energies of the urea group of L1 ligand in TMU-31 in the presence of nitroanaylytes were also studied using DFT method with B3LYP/6-31++G** with diffuse basis functions. The calculated counterpoise corrected interaction energies are summarized in Figure S40, showing that the $_{urea}$N-H$\cdots$O$_{analyte}$ hydrogen bonding interaction (with the $R_2^2(8)$ graph-set motif) energy for ligand L1/NM is -13.48 kcal/mol and is higher than L1/NB (-9.09 kcal/mol), L1/1,3-DNB (-6.89 kcal/mol), L1/2,4-DNT (-7.51 kcal/mol) and L1/TNT (-5.70 kcal/mol) complexes. This shows that, unlike the largest energy offset between the LUMO level of TNT and the CBM of these MOFs, the interaction energy is minimal. Thus, nitro-analytes recognition and fluorescence quenching by TMU-31 and TMU-32 results from a combination of both of these factors. Qualitative support can be obtained by comparing the electrostatic potential maps of the L1 ligand in the presence of NM, NB, 1,3-DNB, 2,4-DNT and TNT. The presence of two electron withdrawing carboxylic acid groups in L1 ligand leads to the polarization of urea N-H fragments and as a consequence of which the Hydrogen bond donating tendency of receptor is enhanced, Figure S41. The electrostatic potential map shows large electronegative region on the oxygen atoms of nitro groups and electropositive region on the hydrogen

atoms of $_{urea}$NH groups, which can be taken as identifiable electropositive and electronegative regions in forming $_{urea}$N-H···$O_{analyte}$ complementary hydrogen bonding interactions. Also, the interaction between the host and the nitromethane guests was investigated by performing Monte Carlo simulations using the adsorption locator module in Accelrys Materials Studio.[69] The simulation reveals that the probable adsorption site for nitromethane guests in these frameworks is near the urea functional group of L1 in TMU-31 and L2 in TMU-32, Figure S42, Table S2.

It is to be noted that besides $_{urea}$N-H···$O_{analyte}$ hydrogen bonds, the flat structures of nitro-analytes also favor π-π stacking interactions with the frameworks. Therefore, it can be suggested that the interaction of nitro-analytes with these frameworks may be a combination of $_{urea}$N-H···$O_{analyte}$ hydrogen bonds and π-π stacking interactions. As described above, in the case of TMU-32, the urea groups are mainly involved in inter-network N-H···O hydrogen bonds, which suggest that π-π stacking interactions along with the $_{urea}$N-H···$O_{analyte}$ hydrogen bonds are presumed to contribute in analyte-MOF interactions. In contrast, it can be stated that urea NH groups of TMU-31 contribute more significantly in the nitro-analyte binding.

Conclusion

Inspired by the previous reports using urea-functionalized MOFs for the activation of nitro groups,[20-22, 25] urea-containing metal-organic frameworks, TMU-31, [Zn(L1)(L2)]•DMF and TMU-32, [Zn(oba)(L2)]•2DMF•H_2O, have been synthesized and structurally characterized by using different techniques. The potential of these frameworks toward nitro-analytes sensing was investigated and compared to each other. The study reveals that the urea groups, inside the pore cavity of MOFs, could be potential binding sites for client nitro-analytes and a combination of $_{urea}$N-H···$O_{analyte}$ hydrogen bonds and π-π stacking interactions are presumed to contribute in analyte-MOF interactions. Also, it was found that the urea groups orientation inside the pore cavity of MOFs and the supramolecular interactions between the interpenetrated networks are important factors in the ability of these frameworks for nitro-substituted compounds sensing.

ASSOCIATED CONTENT

Supporting Information

The Supporting Information is available free of charge on the ACS Publications website at DOI:???

Experimental details, PXRD patterns, TGA, IR spectroscopy and sensing graphs and details (PDF)
Crystallographic data (CIF)

AUTHOR INFORMATION

Corresponding Author

Corresponding Author
*Phone: +98-21-82884416. Fax: +98-21-82884416. E-mail: Morsali_a@modares.ac.ir.
Author Contributions
A.A.T. and L.E. contributed equally to this work.

Notes

The authors declare no competing financial interests.

ACKNOWLEDGMENT

This work was funded by Tarbiat Modares University. DMP acknowledges the Ministry of Education and Science of Russia (Grant 14.B25.31.0005). Aspects of this research were undertaken on the MX1 beamline at the Australian Synchrotron, Victoria, Australia.

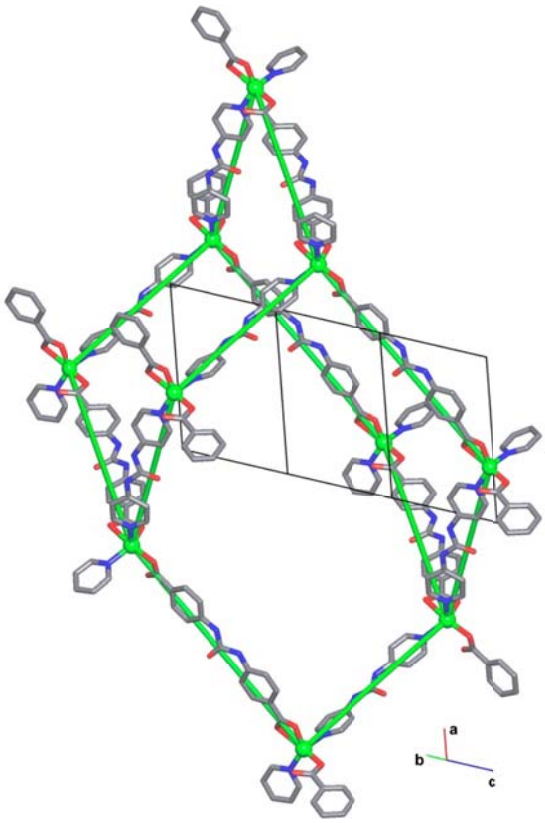

Figure 1. View of a single diamondoid cage of TMU-31 showing the elongation along the *a* axis.

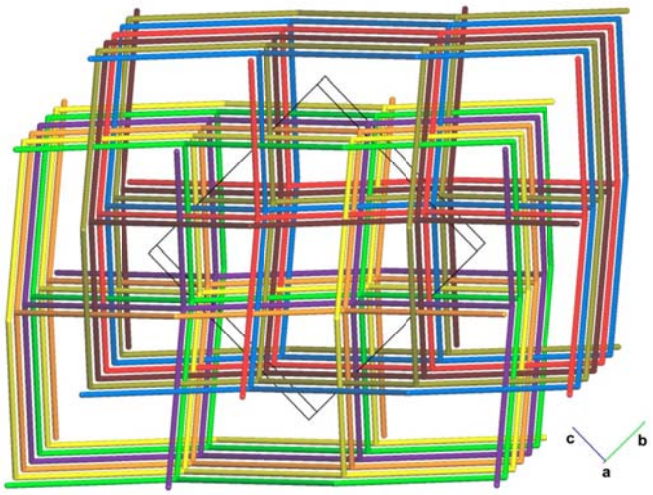

Figure 2. View of the simplified 8-fold interpenetrated **dia** nets of class IIIa in TMU-31 down *a* axes that shows the two 4+4 sets of translationally related nets

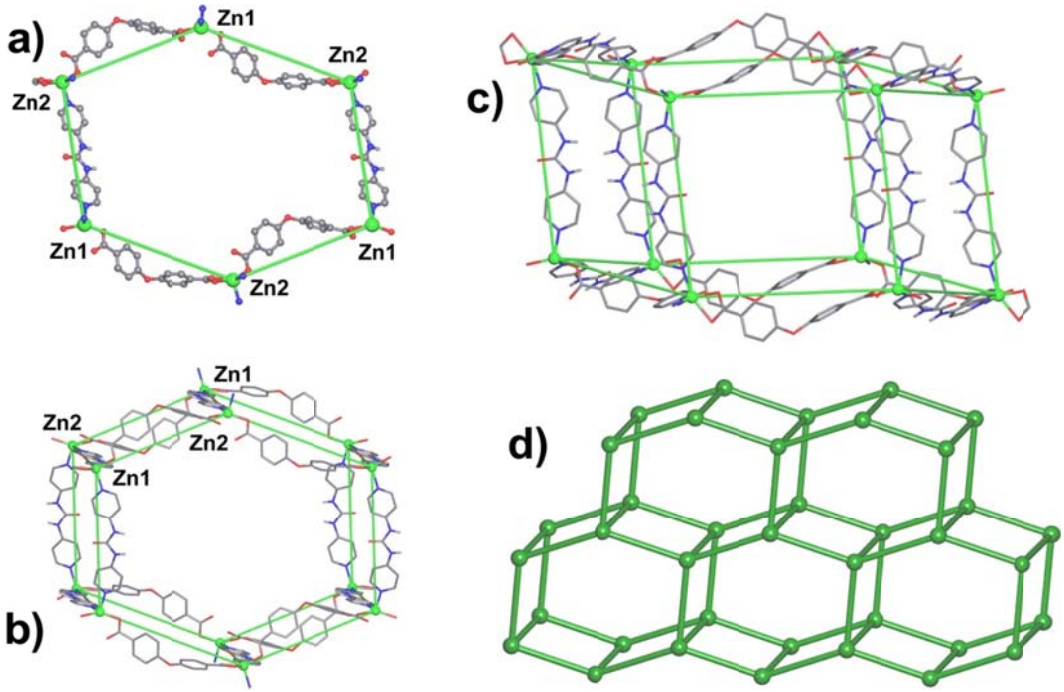

Figure 3. Views of a single thick layer in TMU-32: a) a single hexagonal window composed of alternating Zn1 and Zn2 atoms connected by two L2 and four oba ligands; b) a front view of one hexagonal cage of the thick layer formed by connecting two hexagonal windows by pillaring L2 ligands; c) a lateral view of the same hexagonal cage; d) a single simplified (6,3)Ia layer showing five hexagonal cages.

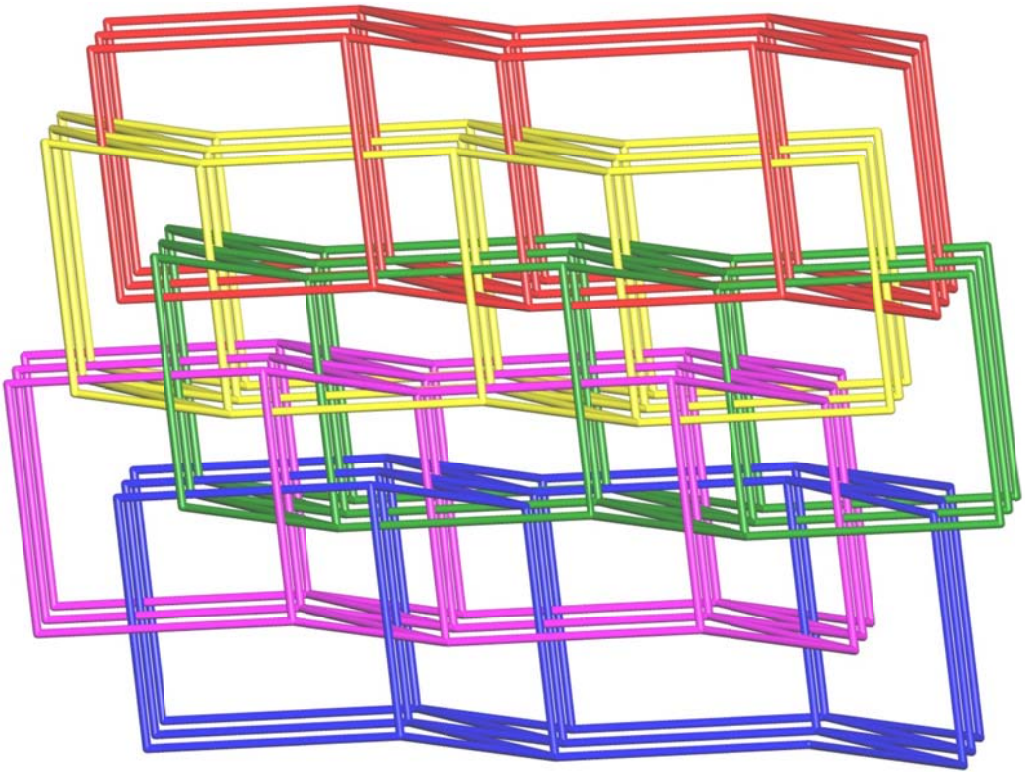

Figure 4. A simplified view of the polycatenated array where one layer (green) is catenated to four others, two above (red and yellow) and two below (purple and blue) giving Doc=4. To separate the whole array in two halves it is necessary to remove two layers (e.g. yellow and green), IS=2.

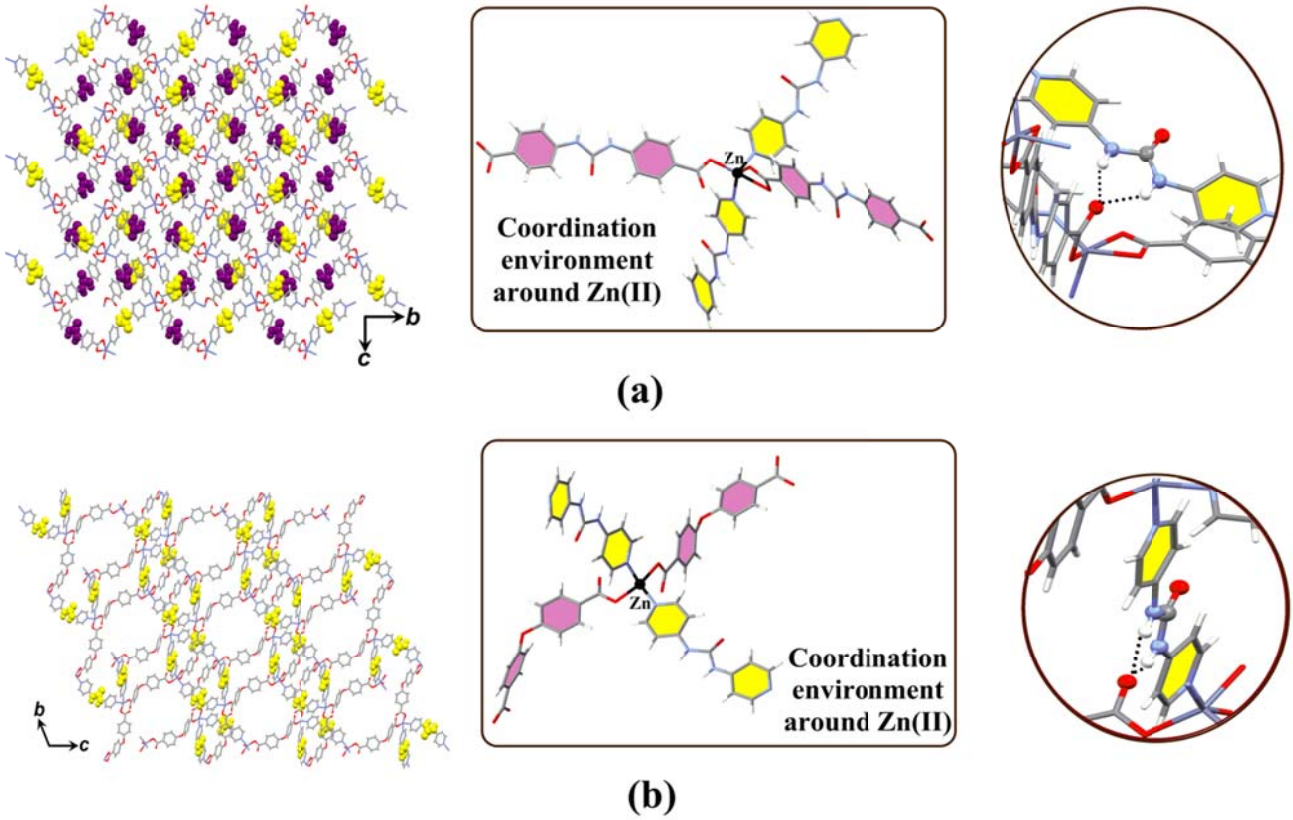

Figure 5. Representation of the three-dimensional structure, coordination environment around Zn(II) and the inter-network hydrogen bonding of TMU-31 (a) and TMU-32 (b). The urea functional groups are shown as space filling models. The yellow urea groups are mainly involved in inter-network H-bonds, while the purple ones represent those that H-bonded to the DMF guest molecules

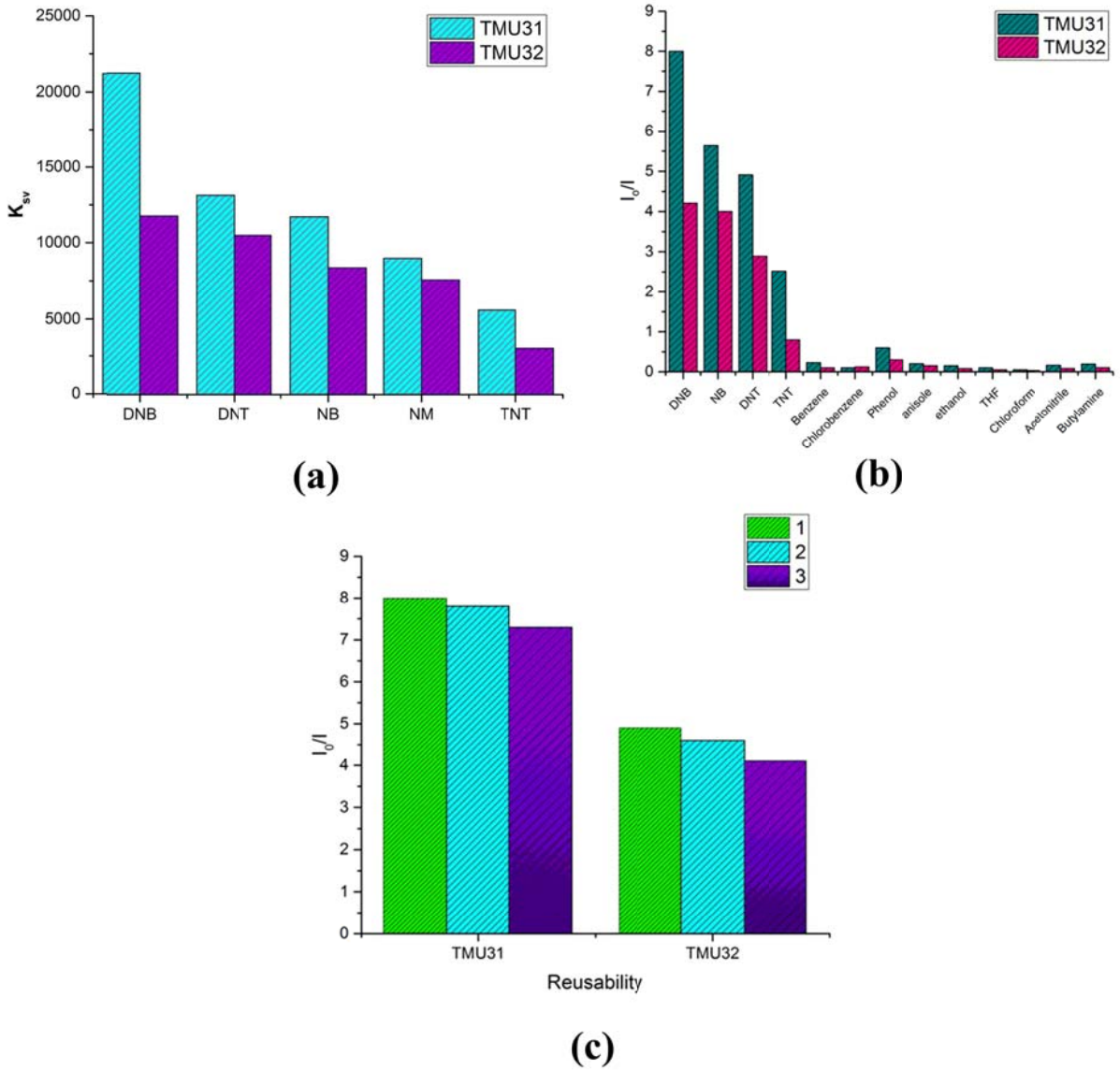

Figure 6. Fluorescence emission spectra of TMU-31 and TMU-32 dispersed in toluene solution of nitroaromatics at different concentrations, excited at 320 nm, comparison of K_{SV} of TMU-31 and TMU-32 towards different nitroaromatics (a) Relative fluorescence response of TMU-31 and TMU-32 to 60 ppm of different organics in toluene (b) Regeneration and reusing of TMU-31 and TMU-32 for nitrobenenze sensing (c)

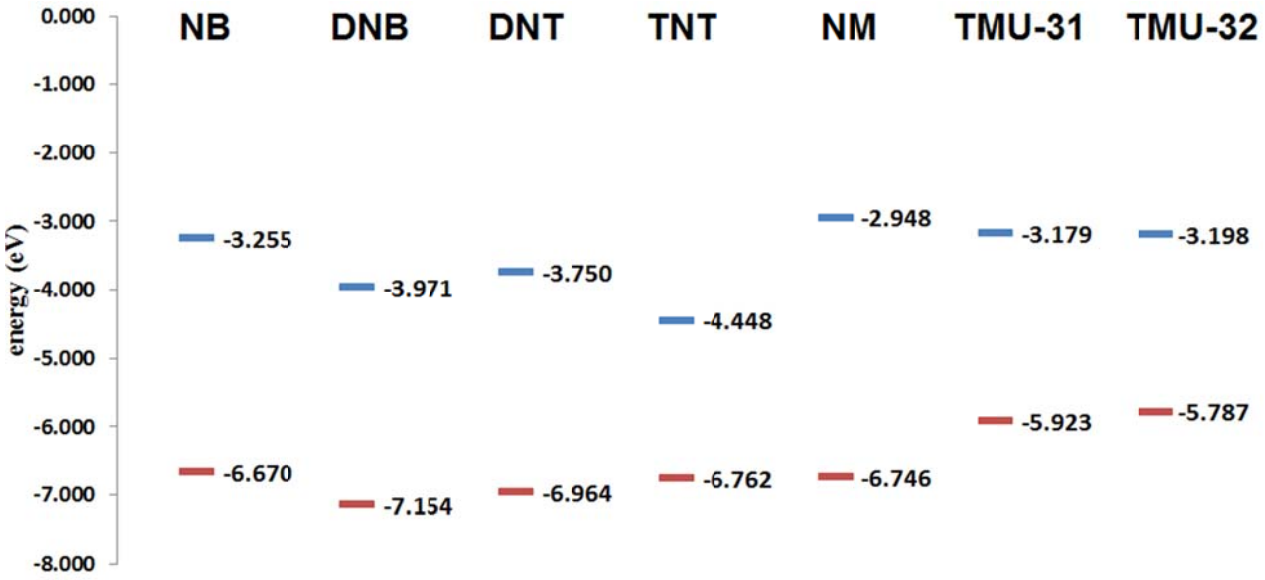

Figure 7. The calculated valence band maximum (VBM) and conduction band minimum (CBM) of TMU-31 and TMU-32 and frontier molecular orbitals of nitrobenzene (NB), 1,3-dinitrobenzene (1,3-DNT), 2,4-dinitrotoluene (2,4-DNT), 2,4,6-trinitrotoluene (TNT) and nitromethane (NM).

REFERENCES

1. Lee, J.; Farha, O. K.; Roberts, J.; Scheidt, K. A.; Nguyen, S. T.; Hupp, J. T., Metal–organic framework materials as catalysts. *Chem Soc Rev* **2009,** *38*, 1450-1459.
2. Li, J.-R.; Sculley, J.; Zhou, H.-C., Metal–organic frameworks for separations. *Chem Rev* **2011,** *112*, 869-932.
3. Kreno, L. E.; Leong, K.; Farha, O. K.; Allendorf, M.; Van Duyne, R. P.; Hupp, J. T., Metal–Organic Framework Materials as Chemical Sensors. *Chem Rev* **2012,** *112*, 1105-1125.
4. Cook, T. R.; Zheng, Y.-R.; Stang, P. J., Metal–Organic Frameworks and Self-Assembled Supramolecular Coordination Complexes: Comparing and Contrasting the Design, Synthesis, and Functionality of Metal–Organic Materials. *Chem Rev* **2013,** *113*, 734-777.
5. Zhang, L.; Kang, Z.; Xin, X.; Sun, D. *CrystEngComm*, **2016**, *18*, 193–206
6. Aboutorabi, L.; Morsali, A.; Tahmasebi, E.; Büyükgüngor, O., Metal–Organic Framework Based on Isonicotinate N-Oxide for Fast and Highly Efficient Aqueous Phase Cr (VI) Adsorption. *Inorg Chem* **2016**.
7. Howarth, A. J.; Wang, T. C.; Al-Juaid, S. S.; Aziz, S. G.; Hupp, J. T.; Farha, O. K., Efficient extraction of sulfate from water using a Zr-metal–organic framework. *Dalton Trans.* **2016,** *45*, 93-97.
8. Abedi, S.; Azhdari Tehrani, A.; Morsali, A., Mechanochemical synthesis of isoreticular metal-organic frameworks and comparative study of their potential for nitrobenzene sensing. *New J Chem* **2015,** *39*, 5108-5111.
9. Liu, D.; Lu, K.; Poon, C.; Lin, W., Metal–organic frameworks as sensory materials and imaging agents. *Inorg Chem* **2013,** *53*, 1916-1924.
10. Lan, A.; Li, K.; Wu, H.; Olson, D. H.; Emge, T. J.; Ki, W.; Hong, M.; Li, J., A luminescent microporous metal–organic framework for the fast and reversible detection of high explosives. *Angew. Chem. Int. Ed.* **2009,** *48*, 2334-2338.
11. Nagarkar, S. S.; Joarder, B.; Chaudhari, A. K.; Mukherjee, S.; Ghosh, S. K., Highly selective detection of nitro explosives by a luminescent metal–organic framework. *Angew. Chem. Int. Ed.* **2013,** *125*, 2953-2957.
12. Balan, B.; Vijayakumar, C.; Tsuji, M.; Saeki, A.; Seki, S., Detection and distinction of DNT and TNT with a fluorescent conjugated polymer using the microwave conductivity technique. *The J. Phys. Chem. B* **2012,** *116*, 10371-10378.
13. Jurcic, M.; Peveler, W. J.; Savory, C. N.; Scanlon, D. O.; Kenyon, A. J.; Parkin, I. P., The vapour phase detection of explosive markers and derivatives using two fluorescent metal–organic frameworks. *J. Mater. Chem. A* **2015,** *3*, 6351-6359.
14. Kim, K., Metal–organic frameworks: Entering the recognition domain. *Nat Chem* **2009,** *1*, 603-604.
15. Karmakar, A.; Kumar, N.; Samanta, P.; Desai, A. V.; Ghosh, S. K., A Post-Synthetically Modified MOF for Selective and Sensitive Aqueous-Phase Detection of Highly Toxic Cyanide Ions. *Chem– Eur. J.* **2016,** *22*, 864-868.
16. Azhdari Tehrani, A.; Abedi, S.; Morsali, A.; Wang, J.; Junk, P. C., Urea-containing metal-organic frameworks as heterogeneous organocatalysts. *J. Mater. Chem. A* **2015,** *3*, 20408-20415.
17. Alegre-Requena, J. V.; Marqués-López, E.; Herrera, R. P.; Díaz, D. D., Metal–organic frameworks (MOFs) bring new life to hydrogen-bonding organocatalysts in confined spaces. *Crystengcomm* **2016,** *18*, 3985-3995.
18. Zhang, X.; Zhang, Z.; Boissonnault, J.; Cohen, S. M., Design and synthesis of squaramide-based MOFs as efficient MOF-supported hydrogen-bonding organocatalysts. *Chem Commun* **2016,** *52*, 8585-8588.

19. Dong, X.-W.; Liu, T.; Hu, Y.-Z.; Liu, X.-Y.; Che, C.-M., Urea postmodified in a metal–organic framework as a catalytically active hydrogen-bond-donating heterogeneous catalyst. *Chem Commun* **2013,** *49*, 7681-7683.
20. McGuirk, C. M.; Katz, M. J.; Stern, C. L.; Sarjeant, A. A.; Hupp, J. T.; Farha, O. K.; Mirkin, C. A., Turning On Catalysis: Incorporation of a Hydrogen-Bond-Donating Squaramide Moiety into a Zr Metal–Organic Framework. *J Am Chem Soc* **2015,** *137*, 919-925.
21. Dong, X.-W.; Liu, T.; Hu, Y.-Z.; Liu, X.-Y.; Che, C.-M., Urea postmodified in a metal–organic framework as a catalytically active hydrogen-bond-donating heterogeneous catalyst. *Chem. Commun.* **2013,** *49*, 7681-7683.
22. Roberts, J. M.; Fini, B. M.; Sarjeant, A. A.; Farha, O. K.; Hupp, J. T.; Scheidt, K. A., Urea metal–organic frameworks as effective and size-selective hydrogen-bond catalysts. *J Am Chem Soc* **2012,** *134*, 3334-3337.
23. Siu, P. W.; Brown, Z. J.; Farha, O. K.; Hupp, J. T.; Scheidt, K. A., A mixed dicarboxylate strut approach to enhancing catalytic activity of a de novo urea derivative of metal–organic framework UiO-67. *Chem Commun* **2013,** *49*, 10920-10922.
24. Luan, Y.; Zheng, N.; Qi, Y.; Tang, J.; Wang, G., Merging metal–organic framework catalysis with organocatalysis: A thiourea functionalized heterogeneous catalyst at the nanoscale. *Catal. Sci. & Techno.* **2014,** *4*, 925-929.
25. Wang, X.-J.; Li, J.; Li, Q.-Y.; Li, P.-Z.; Lu, H.; Lao, Q.; Ni, R.; Shi, Y.; Zhao, Y., A urea decorated (3, 24)-connected rht-type metal–organic framework exhibiting high gas uptake capability and catalytic activity. *Crystengcomm* **2015,** *17*, 4632-4636.
26. Busschaert, N.; Caltagirone, C.; Van Rossom, W.; Gale, P. A., Applications of supramolecular anion recognition. *Chem Rev* **2015,** *115*, 8038-8155.
27. Amendola, V.; Fabbrizzi, L.; Mosca, L., Anion recognition by hydrogen bonding: urea-based receptors. *Chem Soc Rev* **2010,** *39*, 3889-3915.
28. Beer, P. D.; Gale, P. A., Anion recognition and sensing: the state of the art and future perspectives. *Angew. Chem. Int. Ed.,* **2001,** *40*, 486-516.
29. Pandurangan, K.; Kitchen, J. A.; Blasco, S.; Boyle, E. M.; Fitzpatrick, B.; Feeney, M.; Kruger, P. E.; Gunnlaugsson, T., Unexpected Self-Sorting Self-Assembly Formation of a [4: 4] Sulfate: Ligand Cage from a Preorganized Tripodal Urea Ligand. *Angew. Chem. Int. Ed.* **2015,** *54*, 4566-4570.
30. Kirby, I. L.; Pitak, M. B.; Wenzel, M.; Wilson, C.; Sparkes, H. A.; Coles, S. J.; Gale, P. A., Systematic structural analysis of a series of anion receptor complexes. *Crystengcomm* **2013,** *15*, 9003-9010.
31. Forgan, R. S.; Marshall, R. J.; Struckmann, M.; Bleine, A. B.; Long, D.-L.; Bernini, M. C.; Fairen-Jimenez, D., Structure-directing factors when introducing hydrogen bond functionality to metal–organic frameworks. *Crystengcomm* **2015,** *17*, 299-306.
32. Blatov, V. A.; Shevchenko, A. P.; Proserpio, D. M., Applied topological analysis of crystal structures with the program package ToposPro. *Cryst Growth Des* **2014,** *14*, 3576-3586.
33. Cheng, J.-J.; Chang, Y.-T.; Wu, C.-J.; Hsu, Y.-F.; Lin, C.-H.; Proserpio, D. M.; Chen, J.-D., Highly interpenetrated diamondoid nets of Zn (II) and Cd (II) coordination networks from mixed ligands. *Crystengcomm* **2012,** *14*, 537-543.
34. Gong, Y.; Li, J.; Qin, J.; Wu, T.; Cao, R.; Li, J., Metal (II) coordination polymers derived from bis-pyridyl-bis-amide ligands and carboxylates: syntheses, topological structures, and photoluminescence properties. *Cryst Growth Des* **2011,** *11*, 1662-1674.
35. Koch, E.; Fischer, W., Types of sphere packings for crystallographic point groups, rod groups and layer groups. *Z Kristallogr* **1978,** *148*, 107-152.

36. Mitina, T. G.; Blatov, V. A., Topology of 2-periodic coordination networks: toward expert systems in crystal design. *Cryst Growth Des* **2013,** *13*, 1655-1664.
37. Carlucci, L.; Ciani, G.; Proserpio, D. M.; Mitina, T. G.; Blatov, V. A., Entangled two-dimensional coordination networks: a general survey. *Chem Rev* **2014,** *114*, 7557-7580.
38. Carlucci, L.; Ciani, G.; Porta, F.; Proserpio, D. M.; Santagostini, L., Crystal Engineering of Mixed-Metal Ru–Ag Coordination Networks by Using the trans-[RuCl2 (pyz) 4](pyz= pyrazine) Building Block. *Angew. Chem. Int. Ed.* **2002,** *41*, 1907-1911.
39. Post, M.; Trotter, J., Cadmium (II) formate dihydrate. *Acta Crystallogr. Sec. B: Struct. Crystallogr. Cryst. Chem.* **1974,** *30*, 1880-1882.
40. Ju, Z.; Cao, D.; Qin, L.; Zhang, C.; Zhang, M.; Shi, Z.; Zheng, H., Syntheses, characterization, and properties of five coordination compounds based on the ligand tetrakis (4-pyridyloxymethylene) methane. *Crystengcomm* **2014,** *16*, 3917-3925.
41. Korkmaz, N.; Karadağ, A.; Aydın, A.; Yanar, Y.; Karaman, İ.; Tekin, Ş., Synthesis and characterization of two novel dicyanidoargentate (I) complexes containing N-(2-hydroxyethyl) ethylenediamine exhibiting significant biological activity. *New J Chem* **2014,** *38*, 4760-4773.
42. Spek, A. L., Structure validation in chemical crystallography. *Acta Crystallogr. Sec. D: Biol. Crystallogr.* **2009,** *65* (2), 148-155.
43. Naranthatta, M. C.; Das, D.; Tripathy, D.; Sahoo, H. S.; Ramkumar, V.; Chand, D. K., Consequence of Presence and Absence of π-Clouds at Strategic Locations of Designed Binuclear Pd (II) Complexes on Packing: Self-Assembly of Self-Assembly by Intermolecular Locking and Packing. *Cryst Growth Des* **2012,** *12*, 6012-6022.
44. Chandran, S. K.; Thakuria, R.; Nangia, A., Silver (I) complexes of N-4-halophenyl-N′-4-pyridyl ureas. Isostructurality, urea··· nitrate hydrogen bonding, and Ag··· halogen interaction. *Crystengcomm* **2008,** *10*, 1891-1898.
45. Byrne, P.; Lloyd, G. O.; Anderson, K. M.; Clarke, N.; Steed, J. W., Anion hydrogen bond effects in the formation of planar or quintuple helical coordination polymers. *Chem Commun* **2008,** 32, 3720-3722.
46. Custelcean, R.; Haverlock, T. J.; Moyer, B. A., Anion separation by selective crystallization of metal-organic frameworks. *Inorg Chem* **2006,** *45*, 6446-6452.
47. Custelcean, R.; Moyer, B. A.; Bryantsev, V. S.; Hay, B. P., Anion coordination in metal-organic frameworks functionalized with urea hydrogen-bonding groups. *Cryst Growth Des* **2006,** *6*, 555-563.
48. Kirby, I. L.; Pitak, M. B.; Wilson, C.; Gale, P. A.; Coles, S. J., Electron density distribution studies as a tool to explore the behaviour of thiourea-based anion receptors. *Crystengcomm* **2015,** *17*, 2815-2826.
49. Etter, M. C.; Urbanczyk-Lipkowska, Z.; Zia-Ebrahimi, M.; Panunto, T. W., Hydrogen bond-directed cocrystallization and molecular recognition properties of diarylureas. *J Am Chem Soc* **1990,** *112*, 8415-8426.
50. Wood, D. M.; Greenland, B. W.; Acton, A. L.; Rodríguez-Llansola, F.; Murray, C. A.; Cardin, C. J.; Miravet, J. F.; Escuder, B.; Hamley, I. W.; Hayes, W., pH-Tunable Hydrogelators for Water Purification: Structural Optimisation and Evaluation. *Chem–Eur. J.* **2012,** *18*, 2692-2699.
51. Reddy, L. S.; Chandran, S. K.; George, S.; Babu, N. J.; Nangia, A., Crystal Structures of N-Aryl-N′-4-Nitrophenyl Ureas: Molecular Conformation and Weak Interactions Direct the Strong Hydrogen Bond Synthon. *Cryst. Growth & Des.* **2007,** *7*, 2675-2690.

52. Yamashita, A.; Norton, E. B.; Williamson, R. T.; Ho, D. M.; Sinishtaj, S.; Mansour, T. S., Use of Bis-(chiral α-methylbenzyl) glycine Esters for Synthesis of Enantiopure β-Hydroxyamino Esters. *Org Lett* **2003,** *5*, 3305-3308.
53. Toal, S. J.; Sanchez, J. C.; Dugan, R. E.; Trogler, W. C., Visual Detection of Trace Nitroaromatic Explosive Residue Using Photoluminescent Metallole-Containing Polymers. *J. forens. sci.***2007,** *52*, 79-83.
54. Bevers, S.; Schutte, S.; McLaughlin, L. W., Naphthalene-and perylene-based linkers for the stabilization of hairpin triplexes. *J Am Chem Soc* **2000,** *122*, 5905-5915.
55. Shirai, K.; Matsuoka, M.; Fukunishi, K., Fluorescence quenching by intermolecular π–π interactions of 2, 5-bis (N, N-dialkylamino)-3, 6-dicyanopyrazines. *Dyes and Pigments* **1999,** *42*, 95-101.
56. Azhdari Tehrani, A.; Ghasempour, H.; Morsali, A.; Makhloufi, G.; Janiak, C., The effects of extending the π-electron system of pillaring linkers on fluorescence sensing of aromatic compounds in two isoreticular metal-organic frameworks. *Cryst Growth Des* **2015**. *15*, 5543-5547.
57. He, Y.-C.; Zhang, H.-M.; Liu, Y.-Y.; Zhai, Q.-Y.; Shen, Q.-T.; Song, S.-Y.; Ma, J.-F., Luminescent anionic metal–organic framework with potential nitrobenzene sensing. *Cryst Growth Des* **2014,** *14*, 3174-3178.
58. Yi, F.-Y.; Wang, Y.; Li, J.-P.; Wu, D.; Lan, Y.-Q.; Sun, Z.-M., An ultrastable porous metal–organic framework luminescent switch towards aromatic compounds. *Materials Horizons* **2015,** *2*, 245-251.
59. Joarder, B.; Mukherjee, S.; Chaudhari, A. K.; Desai, A. V.; Manna, B.; Ghosh, S. K., Guest-Responsive Function of a Dynamic Metal–Organic Framework with a π Lewis Acidic Pore Surface. *Chemistry–A European Journal* **2014,** *20*, 15303-15308.
60. Banerjee, D.; Hu, Z.; Li, J., Luminescent metal–organic frameworks as explosive sensors. *Dalton T* **2014,** *43*, 10668-10685.
61. Zhu, X.-D.; Li, Y.; Zhou, W.-X.; Liu, R.-M.; Ding, Y.-J.; Lü, J.; Proserpio, D. M., Metal–organic frameworks assembled from flexible alicyclic carboxylate and bipyridyl ligands for sensing of nitroaromatic explosives. *Crystengcomm* **2016**,18, 4530-4537
62. Ghasempour, H.; Azhdari Tehrani, A.; Morsali, A.; Wang, J.; Junk, P. C., Two pillared metal–organic frameworks comprising a long pillar ligand used as fluorescent sensors for nitrobenzene and heterogeneous catalysts for the Knoevenagel condensation reaction. *Crystengcomm* **2016,** *18*, 2463-2468.
63. He, H.; Song, Y.; Sun, F.; Bian, Z.; Gao, L.; Zhu, G., A porous metal–organic framework formed by a V-shaped ligand and Zn (ii) ion with highly selective sensing for nitroaromatic explosives. *J. Mater. Chem. A* **2015,** *3*, 16598-16603.
64. Gole, B.; Bar, A. K.; Mukherjee, P. S., Modification of extended open frameworks with fluorescent tags for sensing explosives: competition between size selectivity and electron deficiency. *Chem–Eur. J.* **2014,** *20*, 2276-2291.
65. Asha, K.; Bhattacharyya, K.; Mandal, S., Discriminative detection of nitro aromatic explosives by a luminescent metal–organic framework. *J. Mater. Chem. C* **2014,** *2*, 10073-10081.
66. He, H.; Song, Y.; Sun, F.; Zhao, N.; Zhu, G., Sorption Properties and Nitroaromatic Explosives Sensing Based on Two Isostructural Metal–Organic Frameworks. *Cryst Growth Des* **2015,** *15*, 2033-2038.
67. Pramanik, S.; Zheng, C.; Zhang, X.; Emge, T. J.; Li, J., New microporous metal− organic framework demonstrating unique selectivity for detection of high explosives and aromatic compounds. *J Am Chem Soc* **2011,** *133*, 4153-4155.

68. Mueller, T.; Ceder, G., A density functional theory study of hydrogen adsorption in MOF-5. *J. Phys. Chem. B* **2005,** *109*, 17974-17983.
69. Barriga, J.; Coto, B.; Fernandez, B., Molecular dynamics study of optimal packing structure of OTS self-assembled monolayers on SiO 2 surfaces. *Tribol. Int.* **2007,** *40*, 960-966.

For Table of Contents Use Only

Urea Metal-organic Frameworks for Nitro-substituted compounds Sensing

Alireza Azhdari Tehrani, Leili Esrafili, Sedigheh Abedi, Ali Morsali, Lucia Carlucci Davide M. Proserpio, Jun Wang, Peter C. Junk, and Tianfu Liu*

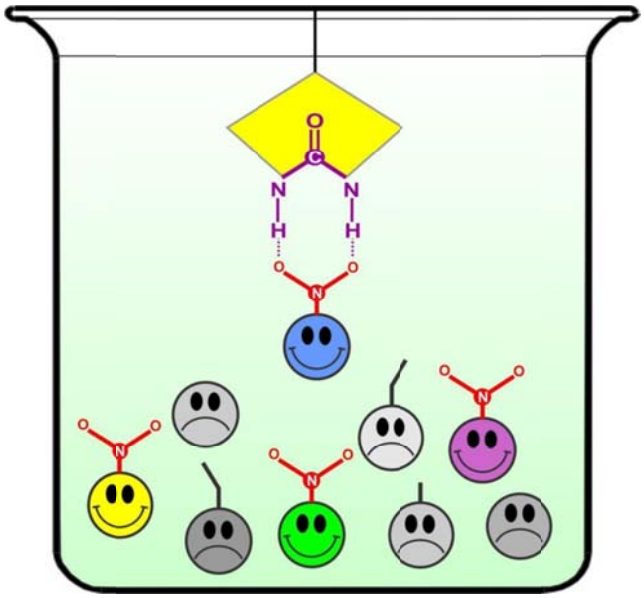

Urea is a particularly interesting building block for designing receptors for neutral or charged guests. Herein, two pillared metal-organic frameworks containing urea functional groups were synthesized and structurally characterized. The sensing properties of these frameworks toward nitro-analytes was investigated and compared to each other. The study reveals the importance of urea groups orientation inside the pore cavity of MOFs, as well as the supramolecular interactions between the interpenetrated networks.